Electronic Supplementary Information

Restraining Lattice Oxygen of Cu_2O by Enhanced Cu-O Hybridization for Selective and Stable Production of Ethylene with CO_2 Electroreduction

Yebo Yao, Yixiang Zhou, Xia Liu, Yongjia Li, Dewei Wang, Xinyue Chi, Xiaoxuan Wang, Rui Zhao, Huiying Zhang, Yanfei Sun, Zhi-Yu Yang, Ying Wei, Yi-Ming Yan*

State Key Lab of Organic−Inorganic Composites, Beijing Advanced Innovation Center for Soft Matter Science and Engineering, Beijing University of Chemical Technology, Beijing, 100029, People's Republic of China

*Corresponding Author.

Email: yanym@mail.buct.edu.cn; bityanyiming@163.com

Experimental Section

Chemicals and Materials

All chemicals were used as received without any further purification. Boric acid (H_3BO_3, ≥99.5%) were purchased from Shanghai Macklin Biochemical Co., Ltd (Shanghai, China). Potassium bicarbonate ($KHCO_3$, ≥99.5%) were purchased from Shanghai Aladdin Biochemical Technology Co., Ltd (Shanghai, China). Ethanol (C_2H_5OH, ≥ 99.7 wt/%), dimethyl sulfoxide (DMSO, ≥ 99.5 wt/%), Copper nitrate trihydrate (Cu $(NO_3)_2 \cdot 3H_2O$), ≥ 99.7 wt/%), sodium hydroxide (NaOH, ≥ 99.6%) were purchased from Beijing Tongguang Fine Chemical Company (Beijing, China).

Preparation of Electrocatalysts

First, the synthesis of B-CuO was reported according to previous published literature.[1] Briefly, 500 mg of Cu $(NO_3)_2$ $6H_2O$ was dissolved in 50 mL of ultrapure distilled water. Then, 1.5 mL of 30% ammonia solution was added to the Cu $(NO_3)_2$ solution under stirring conditions. A blue precipitate of Cu $(OH)_2$ was formed when 10 mL of NaOH solution (1 M) was added dropwise to the abovementioned solutions. The blue precipitate was washed several times with distilled water and then dried overnight in an oven at 60 °C. Then,100 mg of H_3BO_3 was added to the as-synthesized Cu $(OH)_2$ in ethanol solution under stirring conditions. Then, the abovementioned solution was centrifuged and the collected solid products were dried overnight in an oven at 60 °C. The B-CuO sample was obtained by annealing the solid products in an air atmosphere at 500 °C for 2 h. Then, the catalyst ink was prepared by adding 25 mg of catalyst powder with 50 μL of Nafion solution to 10 mL ethanol. The mixture was

ultrasonicated for 30 min. Next, the catalyst ink was sprayed on a carbon paper. At last, the B-Cu_2O sample was obtained by electrochemically reduced at a constant applied potential of -1.4 V for 15 min. For comparation, the synthesis of the undoped Cu_2O was similar to the above process without the addition of boric acid.

Characterizations.

The X-ray diffraction (XRD, Rigaku D/MAX 2550) measurements were performed with Cu Kαradiation (λ=0.15405 nm) to analyze crystalline structures. As for analysis of electrodes after electrolysis, the samples were protected by Ar atmosphere and transferred into vacuum-package prior to XRD measurements. The surface chemical status and composition were acquired by X-ray photoelectron spectroscopy (XPS, Thermo Fisher Scientific) with an Al Kα X-ray as the excitation source. The binding energies obtained in the XPS spectral analysis were corrected for specimen charging by referencing C 1s to 284.8 eV. For in situ XPS tests, the samples after electrolysis were rinsed with deionized water, dried immediately by blowing argon steams and transferred into vacuum-package. Then the catalyst was protected by Ar-steams throughout the sample preparation and evacuated process. XPS depth profiles were obtained with etching of the surface by an Ar-ion beam at an etching rate of ~0.13 nm s^{-1} (taking Ta_2O_5 as reference). A field emission scanning electron microscopy (SEM, FEI Quanta 200), transmission electron microscopy (TEM, FEI Tecnai G2 20) and high-resolution TEM (HRTEM, JEM-2100F, 200 kV) were used to characterize the morphologies and structures of the samples. For imaging of the sample after electrolysis, the catalyst was first loaded onto glassy carbon plate and exfoliated by ultrasonication into ethanol solutions. The HAADF-

STEM images were recorded on a JEOL JEM-ARM200F TEM/STEM with a spherical aberration corrector working at 300 kV. Hydrogen temperature-programmed reduction (H_2-TPR) was investigated by AutoChemII 2920 instrument in a gas mixture of 10% H_2/Ar with a constant flow rate of 50 mL min^{-1}. The O_2-TPD experiments were carried out with the Acquired by Quantachrome TPR Win v3.52. Typically, the catalyst (100 mg) was pretreated at 473 K for 60 min in flowing N_2 (50 mL/min) and then cooled down to 298 K. After pretreatment, the catalyst was saturated in 5% O_2/N_2 mixed gases for 90 min with 30 mL/min, followed by flushing in N_2 (30 mL/min) for 80 min to remove physiosorbed O_2. The O_2-TPD measurement was carried out at 298 to 1183 K in a constant flow of N_2 (50 mL/min) at a heating rate of 10 K/min. As for in situ Raman test, the electrochemical operando cell (EC-RAIR-H) is provided by Beijing Science Star Technology Co. Ltd. An electrolytic cell with three electrode configuration was used for the electrochemical test. A 15 × 15 mm glass carbon electrode loaded with 200 μL catalyst ink was used as working electrode, a graphite rod and Ag/AgCl (saturated KCl) electrodes were used as counter and reference electrode, respectively. The catholyte and anolyte were separated by a proton exchange membrane (117 Dupont). During Raman test, CO_2-saturated 0.1 M $KHCO_3$ was continuously fed into the electrolytic cell at a rate of 10 ml min^{-1}. Raman spectra was collected in the range of 100 to 1000 cm^{-1} using a 532-nm laser. The applied bias was -1.2 V vs. RHE, and other parameters were the same as those used for CO_2RR performance tests. The acquisition time for each spectrum was 10 s.

Electrochemical Measurements.

All the electrochemical measurements were carried out in a three-electrode system. The anodic and cathodic electrolyte compartments were separated by a cation-exchange membrane (Nafion 117 DuPont). Toray carbon paper with an active area of 1 cm^2 was used as working electrode. The counter and reference electrode were the Pt-plate and the Ag/AgCl (in saturated KCl solution) electrode, respectively.

All potentials were measured against an Ag/AgCl reference electrode and converted to the RHE reference scale following the equation:

$$E\ (vs\ RHE) = E\ (vs\ Ag/AgCl) + 0.0197 + (0.0591 \times pH)$$

The working electrode was prepared by the following process: 2.0 mg of samples with 100 μL ethanol. and 10 μL of 5.0 wt. % Nafion solution, followed by sonication for 30 min. Then, 100 μL of catalyst ink was drop-coated on the carbon paper, and the prepared electrodes were dried at ambient atmosphere. The LSV curves were conducted with the CHI 660e electrochemical workstation with a scan rate of 5 mV s^{-1}. Prior to LSV measurements, the 0.5 M $KHCO_3$ electrolyte was purged with Ar- or CO_2- flow for at least 30 min. The controlled potential electrolysis was performed at each potential for 60 min, and the gaseous and liquid products were collected and detected by gas chromatography (TECHCOMP GC7900II) and nuclear magnetic resonance (NMR, Bruker AVANCE AV III 400), respectively. Each reported data point for the CO_2RR experiment was the mean of three consecutive measurements. The gas products from CO_2RR were analyzed using a gas chromatograph equipped with thermal conductivity (TCD) and flame ionization (FID) detectors. For liquid

products, DMSO was used as the internal standard with a chemical shift of 2.6 ppm. The ^{1}H spectrum was measured with water suppression method.

The Faradic efficiencies for gas and liquid products can be calculated as:

Gas products: $FE = (C1 * v * z * F) / (R * j_{total})$

Liquid products: $FE = (C2 * V * z * F) / Q$

C1: Concentration of the gaseous product detected by GC / Vol%

C2: Concentration of the liquid product detected by GC / Vol%

v: CO_2 gas flow rate / L s^{-1}

V: Electrolyte volume / L

z: Charge transfer of the product

F: Faradic Constant / 96485 C mol^{-1}

R: Gas Constant / 22.4 L mol^{-1}

J_{total}: Total current during CO_2 bulk electrolysis / A

Q: All the charge passed during test / C

Computational Details.

DFT calculations were conducted in the Vienna ab initio simulation package (VASP 5.5)[2] with the generalized gradient approximation and the Perdew-Burke-Ernzerhof (PBE) of

exchange-correlation functional.[3] The projector-augment wave (PAW) method was applied to treat the electron-ion interactions with a cut-off energy of 500 eV for the plane-wave basis set to give good converged results.[4] A vacuum space of 15 Å in the z direction is used to avoid the interactions between neighboring slabs. The atomic structures are fully relaxed with a convergence criteria of 1×10^{-5} eV energy difference.

To systematically explore the most stable configurations of reaction intermediates, we modeled and screened a series of configurations of *CO adsorption, protonation and C-C coupling (more calculation details are shown in Figure S11.The Gibbs free energy (G) of absorbed species and gas was calculated as the equation:

$$G = E + ZPE - TS$$

where E is the electronic energy, ZPE is the zero-point energy, and S is entropy.

The charge density difference of B-Cu_2O is defined as:

$$\Delta\rho = \rho_{AB} - \rho_A - \rho_B$$

where ρ_{AB}, ρ_A and ρ_B are the total charge densities of theB-Cu_2O and Cu_2O (111). In calculation of the latter two quantities, the atomic positions are fixed as those they have in the AB system.

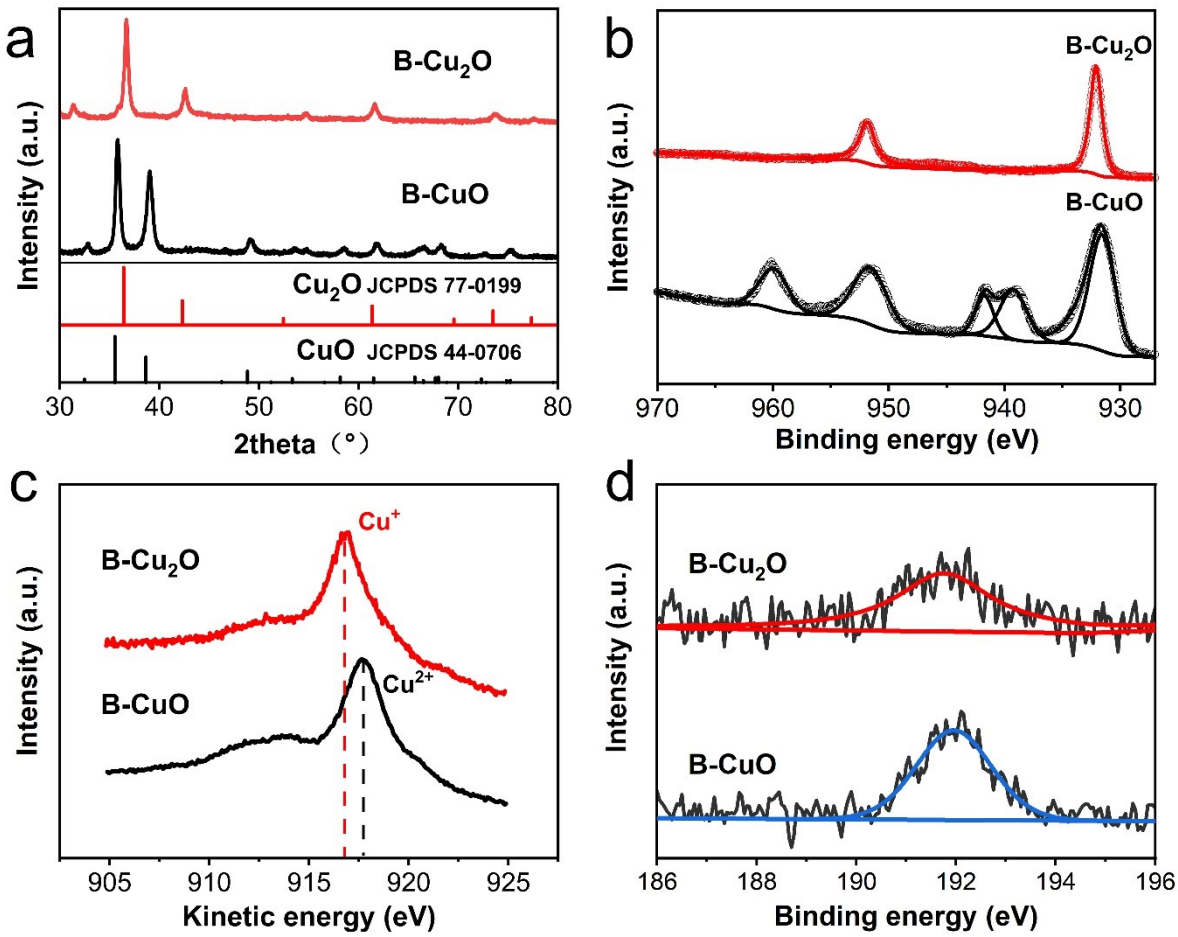

Fig S1. XRD patterns (a) of B-CuO precursor and B-Cu_2O. XPS of (b) Cu 2p, (c) Cu LMM and (d) B 1S spectra for B-CuO precursor and B-Cu_2O.

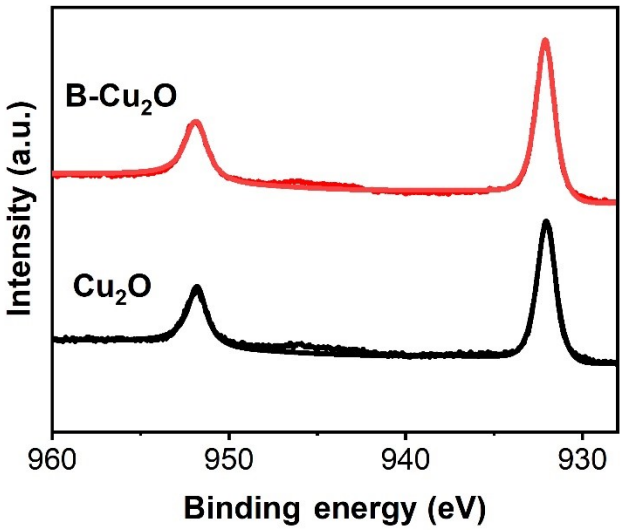

Fig S2. XPS of Cu 2p spectra for B-Cu_2O and undoped Cu_2O.

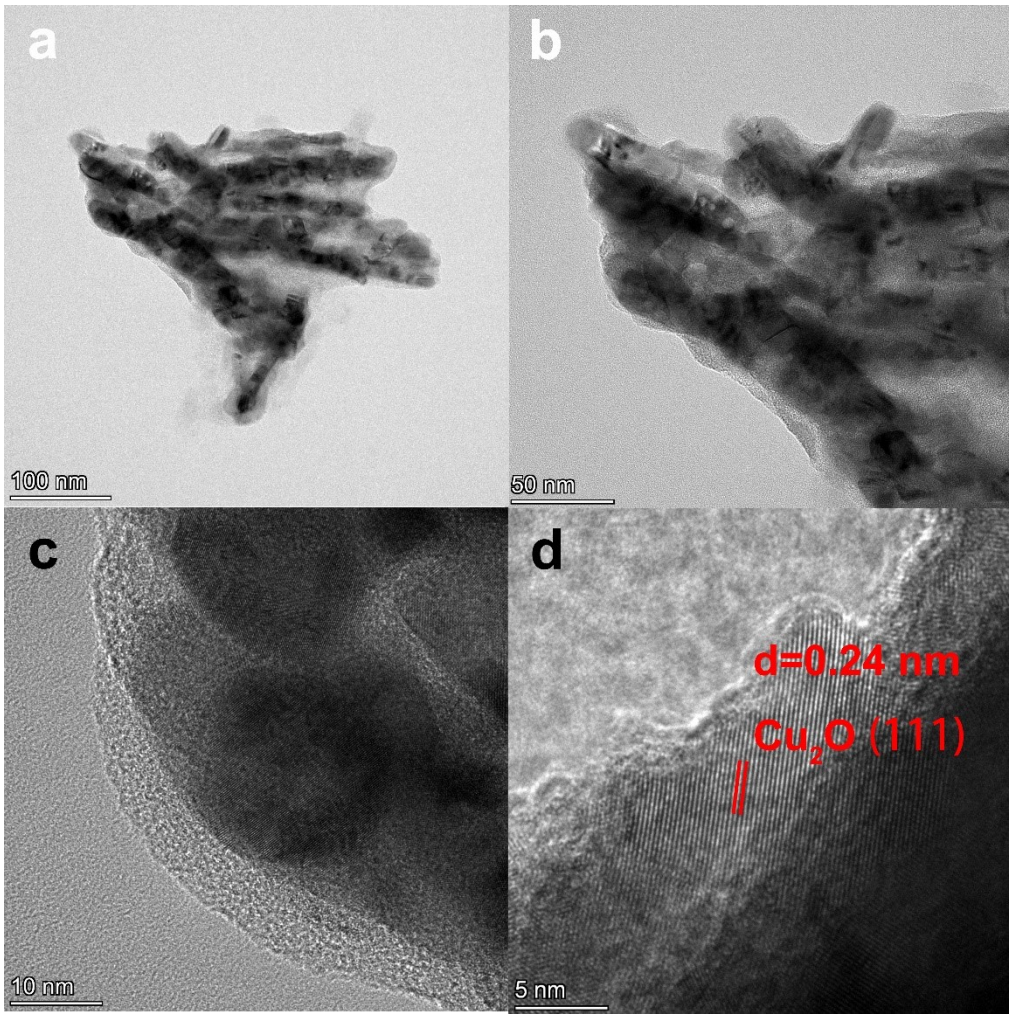

Fig S3. HRTEM (a-d) images of undoped Cu_2O.

a

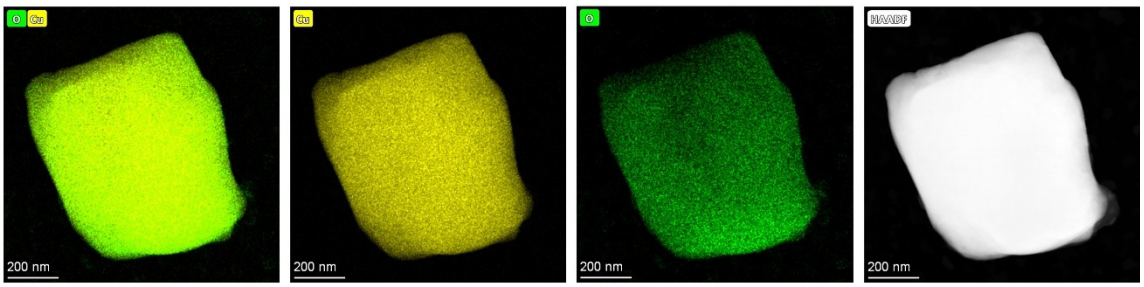

b

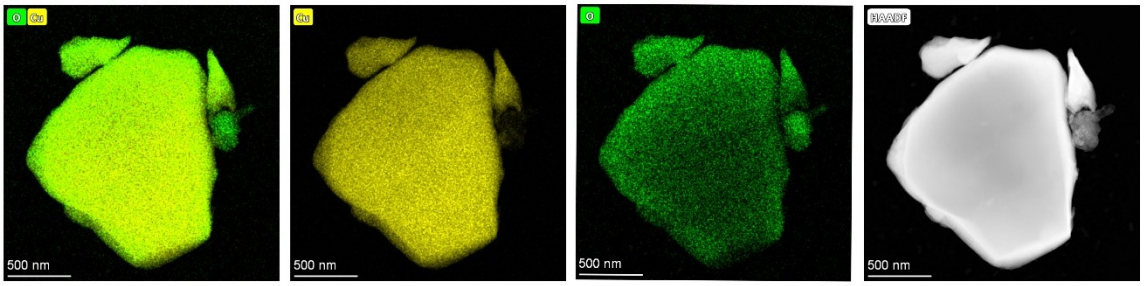

c

Z	Element	Family	Atomic Fraction (%)	Atomic Error (%)	Mass Fraction (%)	Mass Error (%)	Fit error (%)
8	O	K	30.78	5.94	10.07	1.21	0.54
29	Cu	K	69.22	16.23	89.93	16.11	0.04

d

Z	Element	Family	Atomic Fraction (%)	Atomic Error (%)	Mass Fraction (%)	Mass Error (%)	Fit error (%)
8	O	K	20.77	4.29	6.19	0.78	1.51
29	Cu	K	79.23	19.43	93.81	17.14	0.15

Fig S4. Elemental mapping images for undoped Cu_2O before (a) and after 15 min of electrolysis (b) at -1.2 V. EDS spectrum of undoped Cu_2O before (c) and after 15 min of electrolysis (d) at -1.2 V.

a

Z	Element	Family	Atomic Fraction (%)	Atomic Error (%)	Mass Fraction (%)	Mass Error (%)	Fit error (%)
5	B	K	2.52	0.55	0.49	0.06	3.79
8	O	K	12.92	3.79	3.69	0.87	0.32
29	Cu	K	84.56	21.36	95.83	17.70	0.07

b

Z	Element	Family	Atomic Fraction (%)	Atomic Error (%)	Mass Fraction (%)	Mass Error (%)	Fit error (%)
5	B	K	0.88	0.19	0.16	0.02	3.80
8	O	K	11.27	3.34	3.12	0.75	2.01
29	Cu	K	87.85	22.44	96.71	17.94	0.02

Fig S5. EDS spectrum of B-Cu_2O before (a) and after 15 min (b) of electrolysis at -1.2 V.

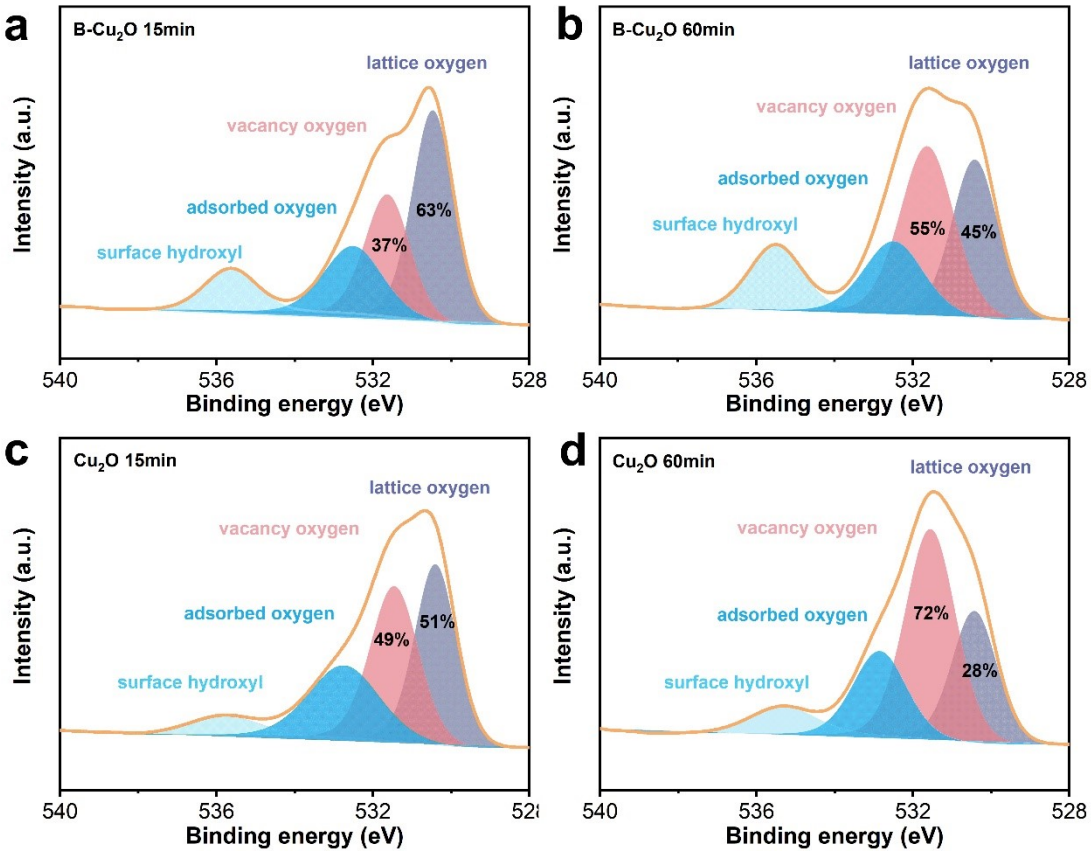

Fig S6. The O 1s spectra for B-Cu_2O after 15 min (a) and 60 min (b) electrolysis at -1.2 V. The O 1s spectra for Cu_2O after 15 min (c) and 60 min (d) electrolysis at -1.2 V.

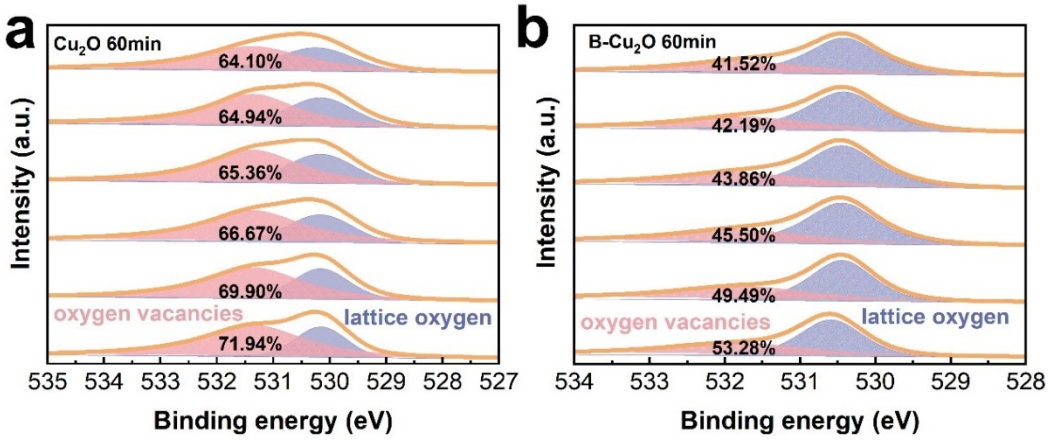

Fig S7. XPS depth profiling analysis for (a) undoped Cu_2O after 60 min of electrolysis, (b) B-Cu_2O after 60 min of electrolysis at -1.2 V.

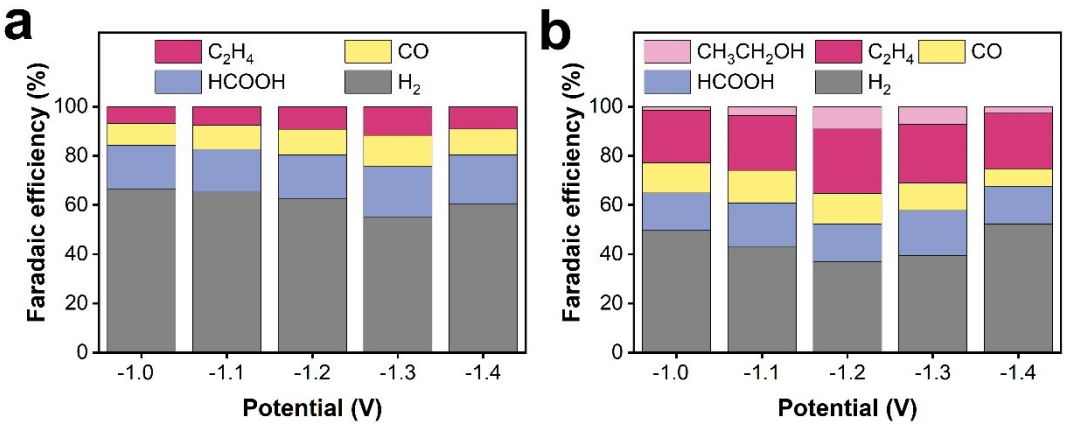

Fig S8. Faradic efficiencies on (a) undoped Cu_2O and (b) B-Cu_2O catalysts at different applied potentials.

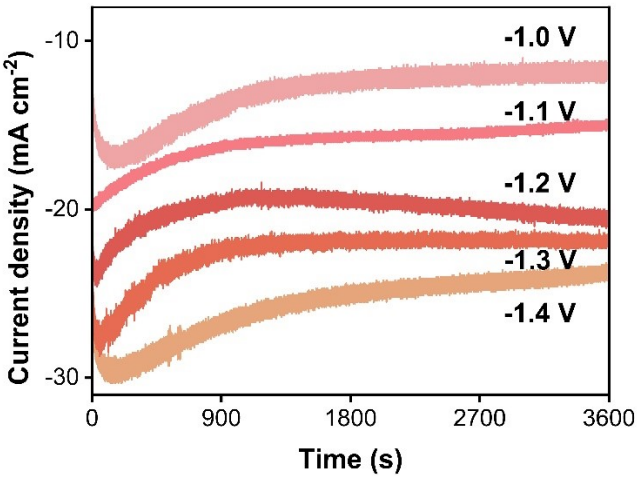

Fig S9. Typical i-t curves at various applied potentials for Cu_2O.

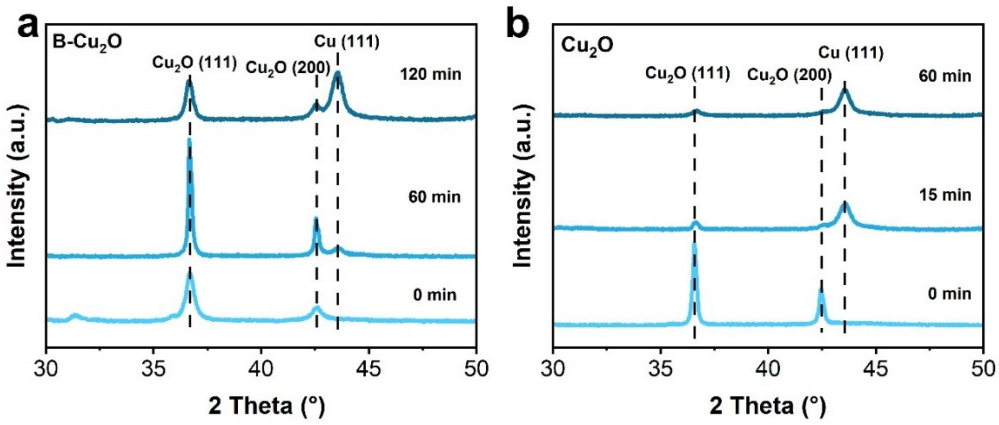

Fig S10. XRD patterns of (a) B-Cu_2O and (b) undoped Cu_2O after different electrolysis time at -1.2 V.

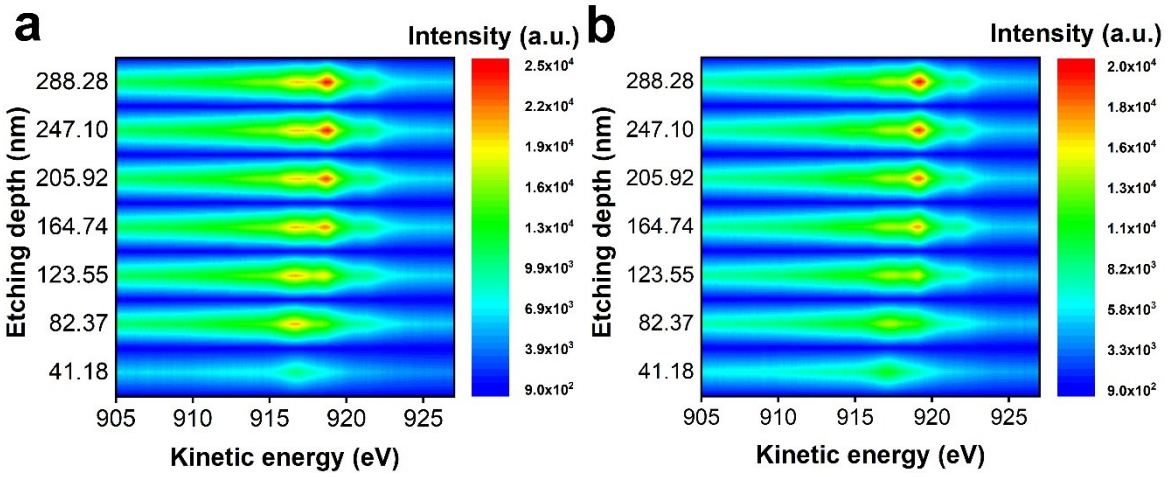

Fig S11. Auger depth profiling analysis for (a) B-Cu_2O after 120 min and (b) undoped Cu_2O after 120 min of electrolysis at -1.2 V showing the surface chemical state with respect to etching depth.

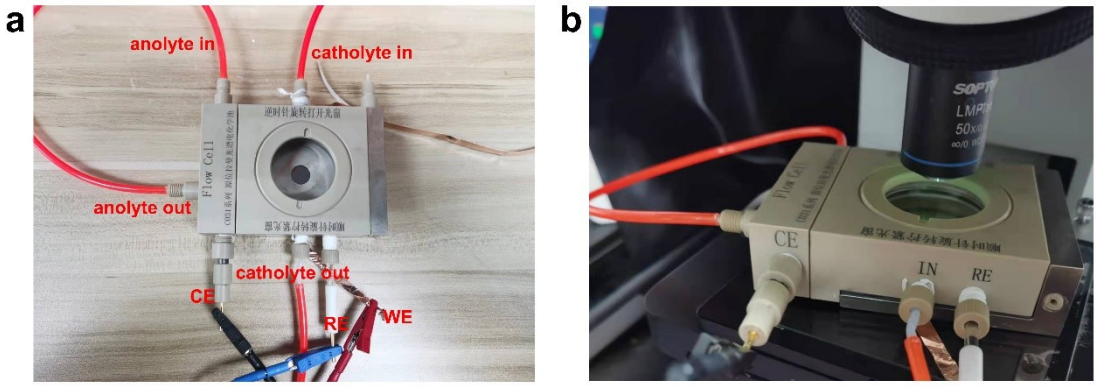

Fig S12. The photographs of in-situ Raman device. (a) Top view of the Raman cell with three electrode system. (b) Side view of the cell under in-situ conditions.

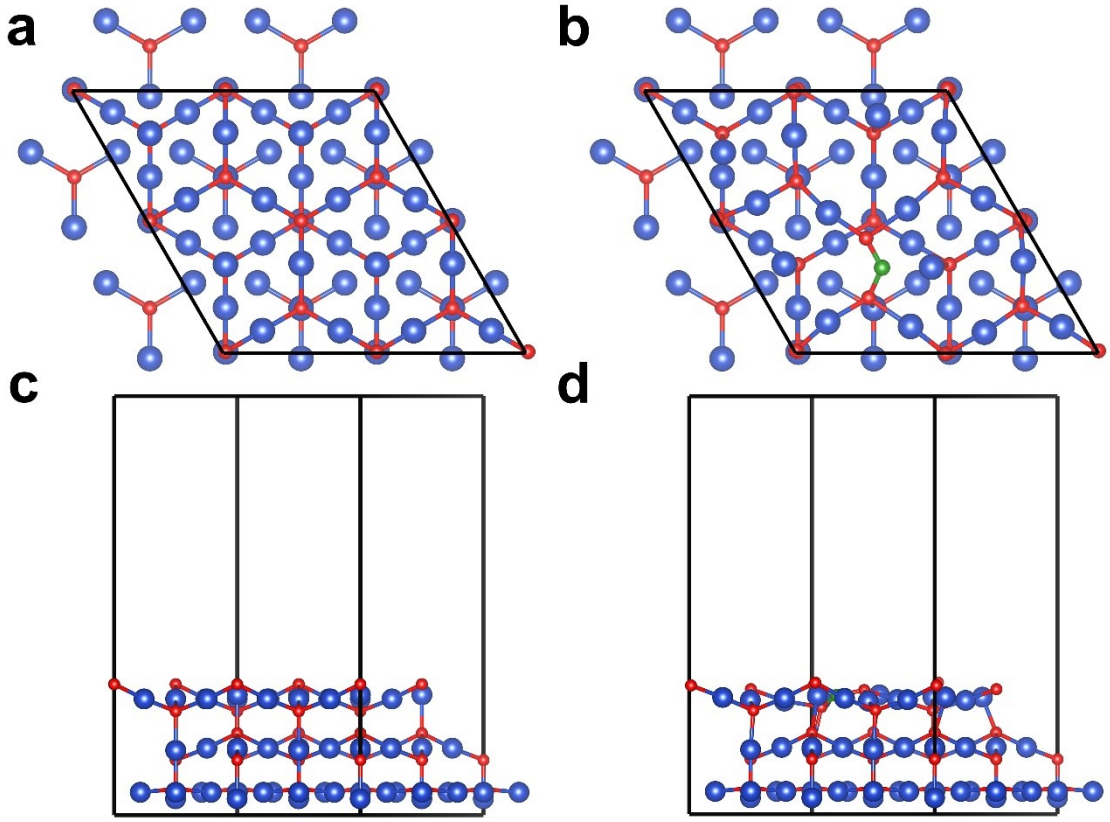

Fig S13. The top view (above) and side view (below) of optimized structure for (a) undoped Cu_2O (111) and (b) B-Cu_2O. Color codes: Cu, blue; O, red; B, green.

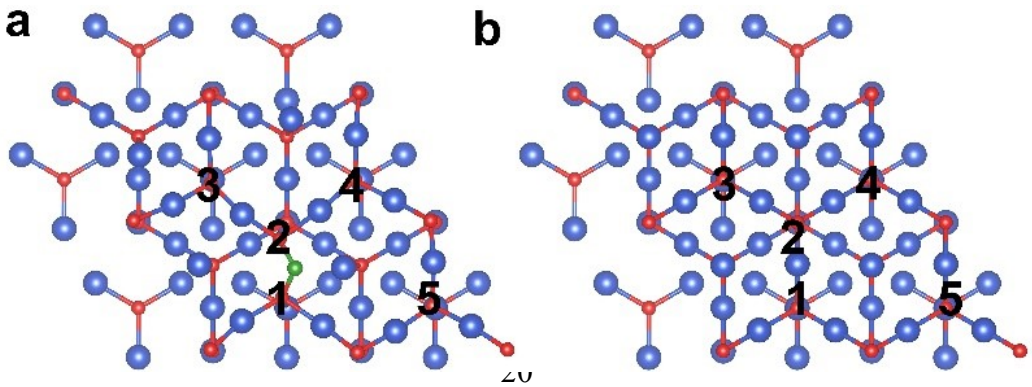

Fig S14. The positions of oxygen vacancy formation in B-Cu_2O and Cu_2O. Color codes: Cu, blue; O, red; B, green.

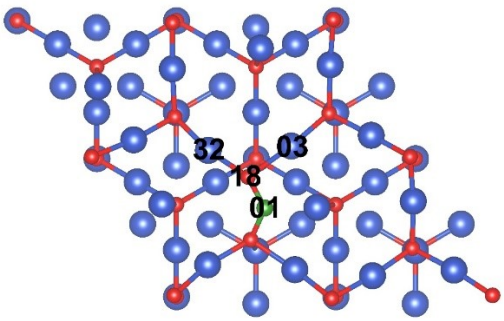

Fig S15. The indexing surface atoms to determine the bond length. Color codes: Cu, blue; O, red; B, green.

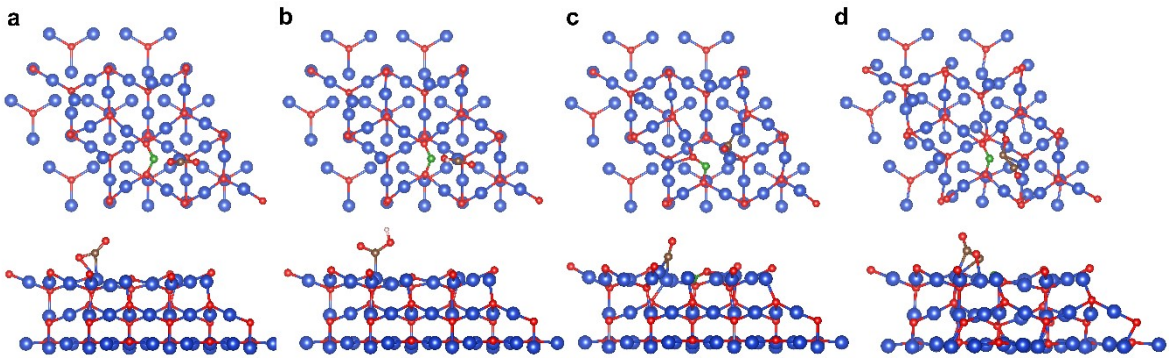

Fig S16. The top view (above) and side view (below) of optimized adsorption configuration for (a) *CO_2, (b) *COOH, (c) *CO and (d) *OCCO intermediates on B-Cu_2O. Color codes: Cu, blue; O, red; B, green; H, white; C, brown.

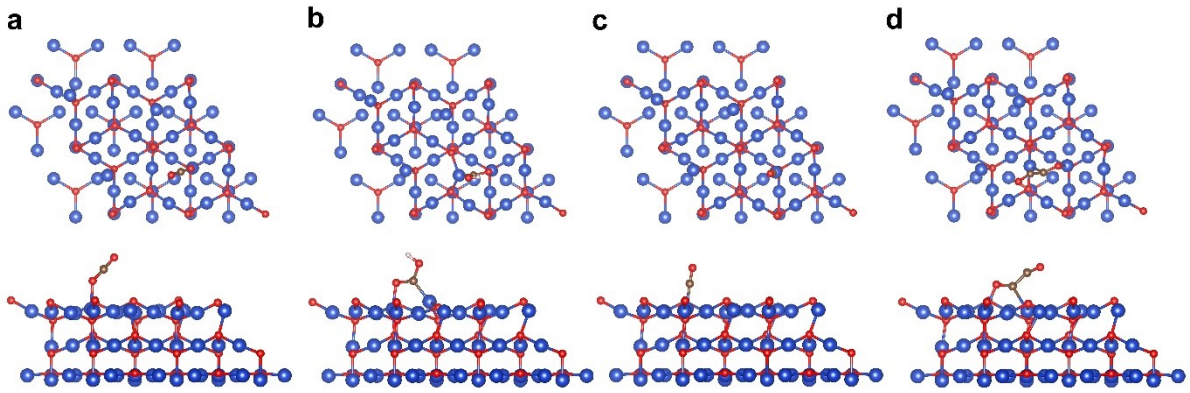

Fig S17. The top view (above) and side view (below) of optimized adsorption configuration for (a) *CO_2, (b) *COOH, (c) *CO and (d) *OCCO intermediates on Cu_2O. Color codes: Cu, blue; O, red; H, white; C, brown.

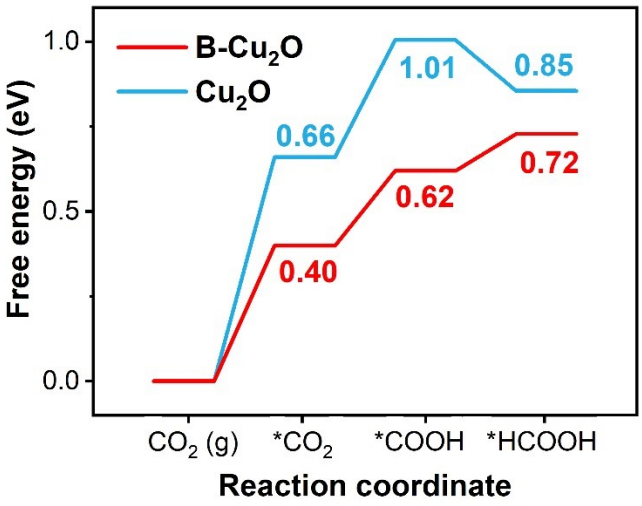

Fig S18. A reaction energy diagram for the CO_2RR to *HCOOH on B-Cu_2O (111) and Cu_2O (111) facets.

Table S1. The amounts of B doping in B-Cu_2O-x investigated by ICP-AES results.

Catalysts	B (wt.%)
B-Cu_2O-1	0
B-Cu_2O-1	0.369
B-Cu_2O-3	0.664
B-Cu_2O-4	1.030

References

1. K. K. Patra, S. Park, H. Song, B. Kim, W. Kim and J. Oh, *ACS Appl. Energy Mater.*, 2020, **3**, 11343-11349.
2. J. F. G. Kresse, *Phys Rev B Condens Matter*, 1996, **16**, 11169-11186.
3. P. E. Blochl, *Phys Rev B Condens Matter,* 1994, **24**, 17953-17979.
4. J. F. G. Kresse, *Com. Mater. Sci.*, 1996, **6**, 1.